H−2 Reactions on Palladium Clusters

ARTICLE *in* THE JOURNAL OF PHYSICAL CHEMISTRY A · AUGUST 2013

Impact Factor: 2.69 · DOI: 10.1021/jp403089x · Source: PubMed

3 AUTHORS:

Adam W. Pelzer
Northwestern University
10 PUBLICATIONS **57** CITATIONS
SEE PROFILE

Julius Jellinek
Argonne National Laboratory
181 PUBLICATIONS **5,675** CITATIONS
SEE PROFILE

Koblar Alan Jackson
Central Michigan University
138 PUBLICATIONS **15,115** CITATIONS
SEE PROFILE

THE JOURNAL OF PHYSICAL CHEMISTRY A

Article

pubs.acs.org/JPCA

H_2 Reactions on Palladium Clusters

Adam W. Pelzer,*[,†,‡,§] Julius Jellinek,*[,†] and Koblar A. Jackson*[,‡,§]

[†]Chemical Sciences and Engineering Division, Argonne National Laboratory, Argonne, Illinois 60439, United States

[‡]Department of Physics, Central Michigan University, Mt. Pleasant, Michigan 48859, United States

[§]Department of Chemical and Biological Engineering, Northwestern University, Evanston, Illinois 60208, United States

Supporting Information

ABSTRACT: Adsorption of an H_2 molecule on Pd_N clusters (N = 2−4, 7, 13, 19, and 55) is investigated using density functional theory with the hybrid PBE0 functional. Low-energy Pd_N isomers, taken from a large pool of candidate structures for all cluster sizes (except N = 55), are used in systematic searches for the most stable Pd_NH_2 (molecular) and Pd_N2H (dissociative) adsorption complexes. Molecular adsorption of H_2 is found to occur strictly at atop sites, with the strongest binding typically occurring at the site with the smallest coordination. Binding of dissociated H atoms occurs preferentially on 3-fold faces and on certain favorable edge sites, while binding at atop sites is unstable. Dissociative adsorption is energetically preferred to molecular adsorption for all cluster sizes. The dissociative adsorption energy decreases with cluster size, with pronounced variations due to cluster size effects for the smallest clusters. Adsorption reaction pathways are computed for cluster sizes up to N = 13. Molecular adsorption is found to be barrierless in all cases. Dissociative adsorption occurs without a barrier for the pathways studied for N = 7 and 13 and with a small barrier on the smaller clusters. Finally, lowest-energy pathways for the migration of a dissociated hydrogen atom between local minima on a cluster surface are computed for the Pd_4, Pd_7, and Pd_{13} clusters. Calculated migration barriers range from 0.05 to 0.25 eV.

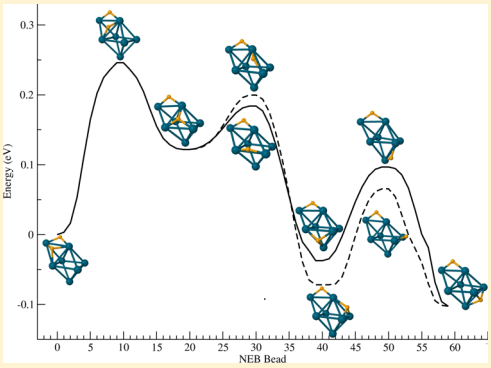

I. INTRODUCTION

Recent experiments have investigated the effectiveness of nanoparticles of palladium and related transition metals, either as single components or as alloys of one or more elements, as catalysts. One reaction of interest is the synthesis of hydrogen peroxide (H_2O_2), an important green oxidant, from gas phase H_2 and O_2 over palladium, mixed palladium/gold, and other metal nanoparticles.[1−3] Experiments have shown that pure Pd nanoparticles were more effective catalysts than pure gold nanoparticles by a factor of 4 but that a 50/50 alloy of Pd/Au outperformed pure Pd by a factor of 2.[4] The composition of the support for the pure and mixed nanoparticles also played a role in the catalytic activity, with TiO_2 supports resulting in a factor of 3 larger output than Al_2O_3 supports.

A key step in hydrogen peroxide catalysis is the breaking of the H_2 bond. The geometry of H_2O_2 features an elongated O−O bond with the H atoms bound at opposite ends of the molecule and separated by nearly 2.5 Å. For this structure to be formed from gas phase reactants, the catalyst must break the H−H bond, bind the O_2, and allow the H atoms to migrate and bind to the O atoms, before the fully formed H_2O_2 molecule can desorb. In this article, we discuss the energetics of H_2 adsorption and the barriers to migration of H atoms on pure Pd_N clusters. This is an important first step in understanding the more complex reactions on mixed and supported clusters. The clusters we examine here, though smaller than the nanoparticles used in experiments, share many relevant features with them. For example, they possess enormous surface area to volume ratios and have low coordinated surface atoms. Pd clusters therefore may be useful as catalysts in their own right. By studying the interaction of H_2 with Pd_N over a large size range using low-energy cluster configurations, we gain insight into the evolution of catalytic behavior with size in these nanosystems.

Previous theoretical work on hydrogen interactions with Pd_N falls into two general categories. The first consists of studies of small clusters containing 1−7 atoms.[5−12] The second involves investigations of palladium surface models[13−17] with the aim of interpreting experimental results on bulk palladium.[18−20] In a recent investigation, nanoparticle size effects were studied by carrying out density functional theory (DFT) calculations on a small series of clusters of increasing size. The cluster structures used in the study were highly symmetric, icosahedral structures that are computationally convenient, but not likely to be the lowest-energy structures at any of the chosen sizes and therefore not necessarily representative of observable Pd clusters, which may involve significantly different atomic arrangements.[21] Here, we present the results of systematic DFT calculations of H_2 adsorption on Pd_N for N = 2−4, 7, 13, 19, and 55. The cluster structures employed were obtained

Received: March 28, 2013
Revised: August 26, 2013
Published: August 27, 2013

   dx.doi.org/10.1021/jp403089x | J. Phys. Chem. A 2013, 117, 10407−10415

from extensive searches for the most stable isomers. The searches were free of symmetry constraints, and many of the resulting structures have low symmetry and a correspondingly rich array of potential binding sites for H_2 molecules. To determine optimal binding sites, we calculated the energetic and structural characteristics for molecular and dissociative adsorption for a large sampling of sites on the most stable Pd_N isomers. For the most stable of these complexes we investigate adsorption barriers and barriers to migration of dissociated H atoms over the cluster surface.

In the following section, we describe the methodology used in this study. We then present and discuss our results in section III. We conclude in section IV with a brief summary.

II. METHODOLOGY

The Pd_N cluster structures used in this study were obtained from extensive searches, free from symmetry constraints, for the most stable isomers and spin multiplicities for N = 2, 3, 4, 7, 13, and 19. The details of these searches are given elsewhere,[22] and only the most stable structures are shown in Figure 1. The coordinates for all of the Pd_N clusters and hydrogenated complexes are given in the Supporting Information.

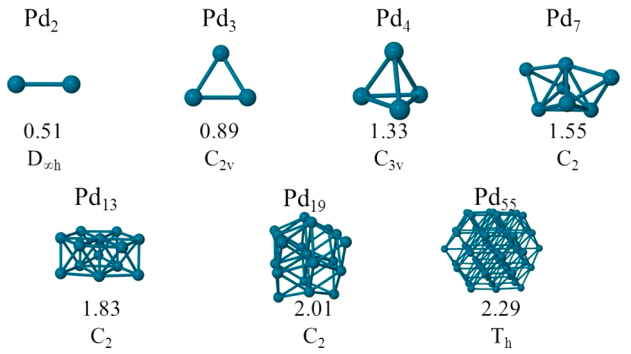

Figure 1. Most stable Pd_N clusters for N = 2, 3, 4, 7, 13, 19, and 55. The cohesive energy ($(E_{tot}(Pd_N) - NE_{tot}(Pd))/N$) is shown in units of eV along with the point group of each cluster.

We investigated H_2 adsorption on several structures/spin states at each N. In most, but not all cases, the most stable adsorption complexes involved the lowest-energy bare cluster isomers. To extend the range of our calculations, we also studied adsorption on Pd_{55}, in this case using only a highly symmetric structure.

To locate the optimal binding sites, an H_2 molecule was systematically placed at a large sampling of symmetry inequivalent edge, atop, and face binding sites on each Pd_N cluster, in at least three independent orientations at each site. For each placement of the dimer, the initial Pd−H distances were approximately 1.7 Å, which is half of the expected Pd−Pd bond length in the large clusters (2.7 Å) plus half of the H−H dimer bond length (0.7 Å). Each starting geometry was then relaxed to a local energy minimum.

Many of the starting configurations resulted in dissociated H atoms when fully relaxed. Additional dissociated configurations were investigated by independently placing two H atoms on the cluster surface at edge and face sites. Atop sites were found to be unfavorable for dissociated H atoms in extensive tests on Pd_2−Pd_4 and were not considered further. For clusters up to N = 13, a large number of symmetry-inequivalent pairings involving edge and face sites were studied. Because of its size, only two binding sites were studied for N = 19, each preserving the C_2 symmetry of the most stable Pd_{19} cluster. These sites were selected to mimic a low-energy adsorption site found for Pd_{13}2H. For N = 55, 8 H atoms were placed symmetrically at face sites to maintain overall T_h symmetry for the adsorption complex. For consistency in energy comparisons, both the complex and the bare cluster were constrained to this symmetry.

At each type of site, the H atom was centered and placed at an approximate distance of 1.7 Å from the Pd atom(s) to which it was bonded. All starting configurations were fully relaxed to local energy minima. All adsorption complexes (both molecular and dissociative) were investigated for M, M+2, and M-2, where M is the ground state multiplicity of the bare cluster. For N = 55, the optimal multiplicity for the bare cluster is M = 19. The Pd_{55}8H complex was relaxed for M = 11, 13, 15, 17, and 19.

All DFT calculations were performed using the NWChem software.[23] A strict SCF convergence criterion of 1×10^{-7} Ha was used for the total energy. The convergence criteria for geometry optimization were set to default values. A normal-mode analysis was performed on all relaxed structures (apart from Pd_{55}), and all geometries were found to be true minima.

A large number of exchange-correlation functionals and basis sets were tested to determine which performed best for Pd-based systems.[22] The PBE0 functional combined with the Stuttgart 18 electron cc-pVDZ-PP ((8s,7p,6d,1f) → [4s,4p,3d,1f]) basis set with a 28 electron effective core potential (ECP) was found to give the best results, and this combination was used for all calculations. Computed and corresponding measured quantities for Pd, Pd_2, and PdH are

Table 1. Calculated Results for Pd, Pd_2, Pd_2^-, and PdH Obtained with the PBE0 Functional and the cc-pVDZ-PP Basis[a]

	IP (eV)	EA (eV)	BE (eV)	R (Å)	ω (cm^{-1})
Pd	8.38	0.56			
	8.3365 ± 0.0001[b]	*0.56214 ± 0.00012*[c]			
Pd_2	7.41	1.31	1.01	2.47	212
	7.7 ± 0.3[d]	*1.30 ± 0.15*[g]	*1.03 ± 0.16*[e]	*2.48*[b]	*210 ± 10*[e]
Pd_2^-			2.15	2.44	222
			2.15 ± 0.17[e]		*206 ± 15*[e]
PdH	8.89		2.36	1.54	2039
	8.81[h]		*2.38 ± 0.3*[h]	*1.53*[i]	

[a]The cc-pVQZ-PP basis set was used for the Pd atom electron affinity calculations. Experimentally observed results are shown in italics for comparison. The ionization potential (IP), electron affinity (EA), binding energy (BE), equilibrium bond length (R), and vibrational frequency (ω) are shown. [b]Ref 24. [c]Ref 25. [d]Ref 26. [e]Ref 27. [f]Ref 28. [g]Ref 29. [h]Ref 30. [i]Ref 31.

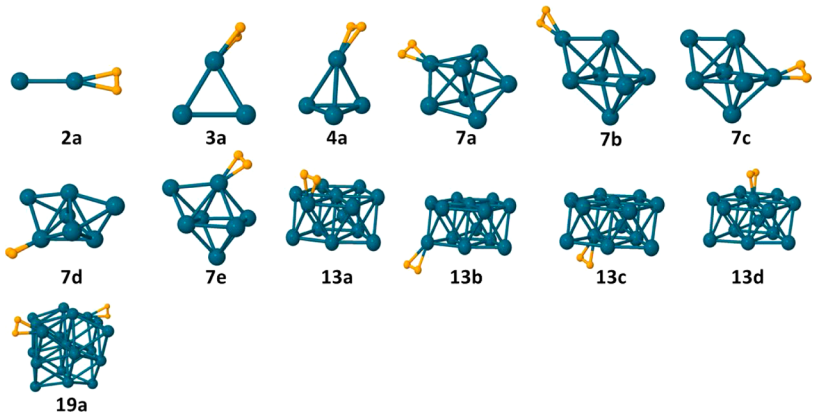

Figure 2. Pd_NH_2 (molecularly adsorbed) complexes. The labels a, b, etc., are in order of decreasing stability for each *N*. Properties for these complexes are given in Table 2

Table 2. Properties of Molecularly Adsorbed Complexes, Pd_NH_2; See Text for Details

	Pd coord	E_{ads} (eV)	$\langle r_{H-H}\rangle$ (Å)	$\langle r_{Pd-H}\rangle$ (Å)	Q_{H2} (e)	ω_{H2} (cm^{-1})
2a	1	0.22	0.80	1.87	−0.01	3534
3a	2	0.33	0.84	1.74	−0.02	3208
4a	3	0.32	0.83	1.78	−0.01	3166
7a	4	0.61	0.86	1.72	0.02	2874
7b	3	0.48	0.85	1.72	0.03	2919
7c	4	0.47	0.85	1.73	0.01	2924
7d	5	0.38	0.84	1.75	0.01	3010
7e	5	0.37	0.85	1.75	0.00	2889
13a	5	0.52	0.88	1.71	0.03	2714
13b	4	0.38	0.84	1.74	0.04	3030
13c	7	0.37	0.85	1.78	0.05	3008
13d	9	0.32	0.85	1.77	0.03	2920
19a	4	0.32	0.83	1.76	0.05	3132

compared in Table 1. The agreement between the PBE0 result and experiment is very good in all cases.

Two key values that characterize an adsorption reaction are the adsorption energy (E_{ads}) and the height of the energy barrier that must be overcome for adsorption to take place. The adsorption energy per H_2 is defined as

$$E_{ads} = [E(Pd_N) + mE(H_2) - E(Pd_NH_{2m})]/m \quad (1)$$

where *m* is the number of H_2 molecules adsorbed on the cluster. All energies in eq 1 include zero-point vibrational contributions (except for $N = 55$). The bare cluster energy $E(Pd_N)$ refers to the energy of the cluster packing present in the adsorbed complex $E(Pd_NH_{2m})$, which may not be the lowest energy cluster for that *N*. Adsorption barriers are found using the nudged elastic band (NEB) method.[32−34] NEB requires as input the geometries corresponding to the reactant and product states. The algorithm then determines the lowest-energy path between these end points through an iterative process. For H_2 adsorption, the product end point was taken to be the relaxed configuration of the adsorption complex, and the reactant end point a configuration in which the H_2 is positioned directly above the adsorption site, far enough away that the interaction between the cluster and the H_2 is effectively zero.

NEB was also used to determine barriers to the migration of dissociated H atoms between neighboring minima in Pd_N2H complexes. For these cases, the relaxed geometries of the neighboring minima were used as end points for a first NEB calculation. The resulting path extends over an energy barrier separating the minima. We then used the geometry corresponding to the peak of the barrier as an initial guess for a saddle point search. Once the saddle point geometry was identified, the original NEB calculation was split into two independent parts: one connecting the initial state to the saddle point and the second extending from the saddle point to the final state. By using three fixed points rather than two in this way, a smoother minimum energy migration path was obtained.

The natural bond orbital (NBO) analysis[35] was used to determine the charge transfer associated with H_2 adsorption.

III. RESULTS AND DISCUSSION

A. Pd_NH_2: Molecular Adsorption. The most stable molecular adsorption complexes found in this study are shown in Figure 2. Lower case letters (a, b, c, etc.) are used to label the complexes for a given size in order of decreasing stability. All stable molecular adsorption occurs at atop sites, where two Pd−H bonds are formed. For $N = 7$, the most stable complex, 7a, involves the second most stable bare cluster packing, while 7b, 7c, and 7e all involve the third most stable cluster packing.[22] Only 7d involves the ground state packing of the bare cluster.

The energetic and structural properties for the Pd_NH_2 complexes shown in Figure 2 are given in Table 2. (For $N = 19$, the results shown are averages for two H_2 dimers placed on the cluster simultaneously to preserve symmetry.) Adsorption energies (E_{ads}) range from 0.22 to 0.61 eV. H−H bond distances range from 0.80 to 0.88 Å, longer than in a free H_2

dx.doi.org/10.1021/jp403089x | J. Phys. Chem. A 2013, 117, 10407−10415

molecule (0.74 Å), and Pd−H bond lengths range from 1.71 to 1.87 Å. A clear trend links longer H−H bonds and shorter Pd−H bonds with larger values of E_{ads}. Similarly, the H−H vibrational stretch mode frequencies in the complexes are somewhat softer (2714 to 3534 cm^{-1}) than in free H_2 (4380 cm^{-1}), and softer modes are correlated with larger adsorption energies. Very limited charge transfer is found for the molecularly adsorbed complexes. For clusters larger than N = 4, electron charge is transferred from the H atoms to Pd_N, leaving the adsorbed dimer slightly positively charged. The ground state spin multiplicities of the adsorption complexes are the same as those of the corresponding bare clusters for all cases studied.

For a given cluster, the surface atoms with the lowest coordination (fewest bonds to other Pd atoms) are generally associated with the largest values of E_{ads}. A typical result can be seen in Table 2 for 7b, 7c, and 7e, all of which involve the same bare cluster packing. The trend does not hold absolutely across packings (cf. 7a and 7b), and there are also a few exceptions for a given packing (cf. 13a and 13b). Still, the trend holds for nearly all the complexes we investigated including those not shown in Figure 2. One implication of this trend is that molecular adsorption is more likely to occur on nanoparticle edges or steps, where the surface Pd atoms are less coordinated than near the center of facets.

Changes in Pd−Pd bond lengths at or near the molecular adsorption site are generally less than 0.1 Å for the clusters studied here, though in the most strongly adsorbed cases (7a and 13a) adjacent bond lengths can be elongated or contracted by as much as 0.2 Å.

The results for molecular adsorption shown in Table 2 are consistent with previous calculations for small Pd clusters. For example, E_{ads} for Pd_4, 0.32 eV, is intermediate between the values found in ref 7, 0.38 eV, and in ref 11, 0.27 eV, while ref 12 gives 0.32 eV as well.

B. Pd_N2H: Dissociative Adsorption. Figure 3 displays the three most stable dissociative adsorption complexes, Pd_N2H, obtained for each cluster size, and Table 3 lists properties calculated for each complex. As seen in the figure, the dissociated H atoms generally occupy face sites in the most stable complexes, although in 7A−C and 13C one of the H atoms is located on an edge site. Pd−H bond lengths for H atoms on face sites range from 1.75 to 1.80 Å for all cluster sizes. The bonds are somewhat shorter at edge sites, 1.65 to 1.7 Å. NBO analysis shows that dissociative adsorption involves a transfer of electron charge from the Pd_N cluster to the H atoms. There is generally more charge transfer to H atoms bound at faces than at edges. The total charge transfer is in the range 0.14 to 0.26 e for most of the complexes, with lower values corresponding to complexes with two edge-bound H atoms. Exceptions to this are the complexes 7A−C and 13C, which have larger charge transfer to edge-bound H atoms and larger net charge transfer overall. These cases are discussed further below.

Dissociative adsorption of an H_2 generally decreases the ground state spin multiplicity from M to $M - 2$, where M is the multiplicity of the bare cluster. This corresponds to a reduction of the number of unpaired spins on the cluster by two in forming bonds to the two H atoms. Note that in the case of N = 55, the reduction is from M = 19 to M = 11, corresponding to a reduction of 8 unpaired spins with the adsorption of 8 H atoms. The exception to this in Table 3 is N = 7, where M = 3 for both the bare cluster and the $Pd_7$2H complex. In this case, there is a near degeneracy between the bare clusters with M = 5 and M = 3, the triplet structure being lower by only 0.01 eV. At all other sizes, the energy difference between the lowest and next-lowest spin multiplicity is at least 0.15 eV.[22]

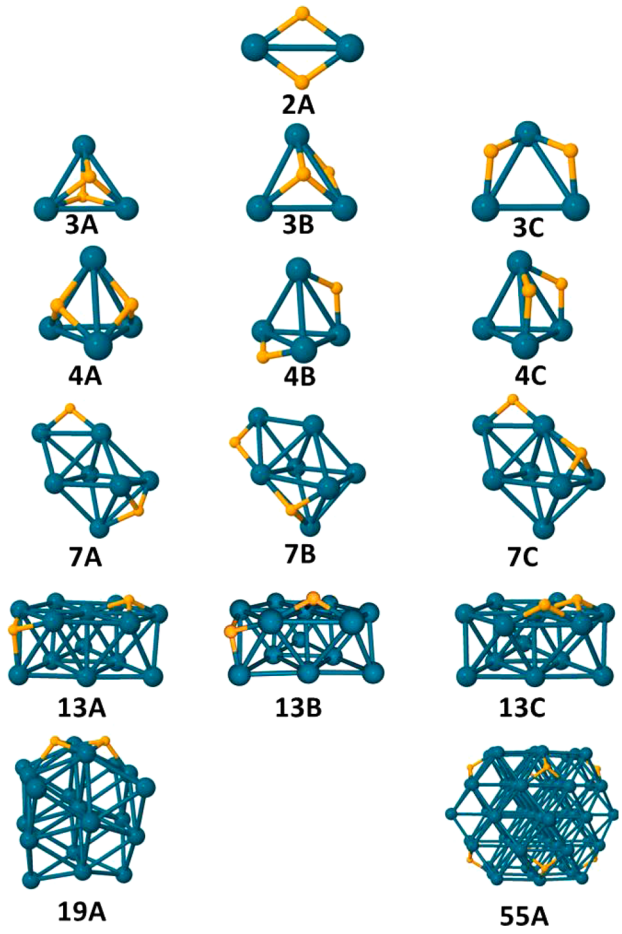

Figure 3. Pd_N2H (dissociatively adsorbed) complexes. The complexes are labeled A, B, etc., in order of decreasing stability. Properties for these complexes are given in Table 3

Changes in Pd−Pd bond lengths after hydrogen adsorption vary with binding configuration (H atom bound to an edge versus a face) and with the size of the cluster. For N = 2−7, the effect of H adsorption is to increase the Pd−Pd distance for all palladium atoms adjacent to the bound hydrogen, with edge-bound H atoms increasing the distance by around 0.2 Å. H atoms bound to a 3-fold face increase the length of the bonds making up the face by between 0.05 and 0.16 Å depending on the proximity of the second hydrogen atom. For the three cases shown in Figure 3 for Pd_{13}, some bonds adjacent to adsorption sites lengthen (up to 0.26 Å), while some contract (up to −0.12 Å). For Pd_{19}, Pd−Pd bonds adjacent to the bound H atoms increase by 0.08 Å or less, and for Pd_{55}, these values decrease by 0.01 Å.

The results for E_{ads} shown in Table 3 are in general agreement with earlier calculations for small Pd_N2H adsorption complexes. For example, E_{ads} for Pd_4 is 0.94 eV, compared to 0.91, 1.13, 0.96, and 1.00 eV in refs 7, 10, 11, and 12, respectively.

C. Favorable Edge Sites and H−H Proximity Effects. As mentioned above, face−face configurations are generally more stable than face−edge or edge−edge configurations in the large number of Pd_N2H complexes we studied. In some cases,

dx.doi.org/10.1021/jp403089x | J. Phys. Chem. A 2013, 117, 10407−10415

Table 3. Computed Properties for the Pd_N2H Dissociative Adsorption Complexes Shown in Figure 3; See Text for Details

			H on face		H on edge		Pd_N
	E_{ads}	$M_i \rightarrow M_f$	Q_H (e)	$\langle r_{Pd-H} \rangle$ (Å)	Q_H (e)	$\langle r_{Pd-H} \rangle$ (Å)	Q_{Pd} (e)
2A	1.72	3 → 1			−0.13	1.67	0.26
3A	1.68	3 → 1	−0.12	1.81			0.24
3B	1.62	3 → 1	−0.17	1.79	−0.08	1.66	0.25
3C	1.51	3 → 1			−0.10	1.66	0.20
4A	0.94	3 → 1	−0.13	1.75			0.26
4B	0.90	3 → 1			−0.09	1.64	0.18
4C	0.65	3 → 1			−0.07	1.65	0.14
7A	1.26	3 → 3	−0.20	1.78	−0.18	1.70	0.38
7B	1.24	3 → 3	−0.19	1.78	−0.18	1.70	0.37
7C	1.22	3 → 3	−0.17	1.77	−0.18	1.70	0.35
13A	0.97	7 → 5	−0.13	1.77			0.26
13B	0.94	7 → 5	−0.15	1.79			0.30
13C	0.87	7 → 5	−0.22	1.77	−0.14	1.70	0.36
19A	0.70	9 → 7	−0.08	1.80			0.16
55A	0.64	19 → 11		1.80			

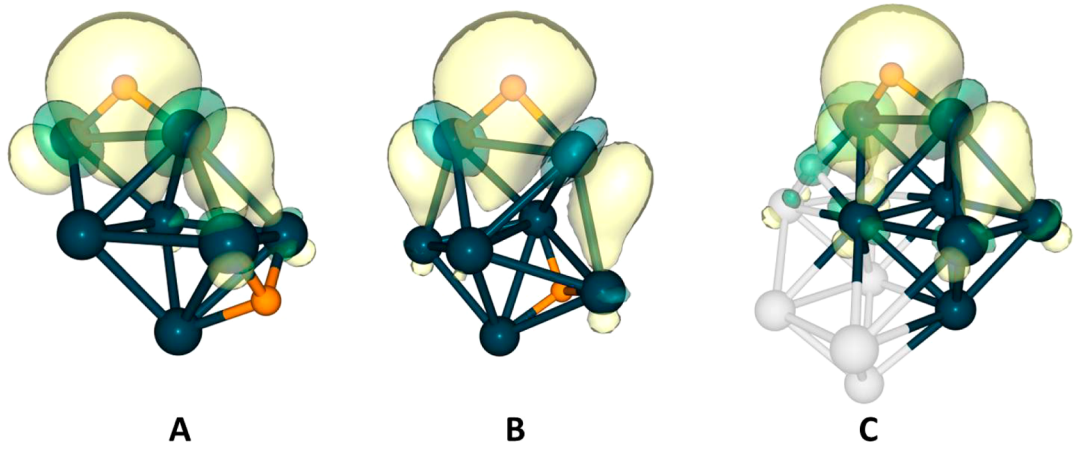

Figure 4. Isosurface plots of the bonding molecular orbitals for an edge bound hydrogen atom in three different adsorption complexes. See text for details.

however, particularly stable face−edge configurations exist. Examples of such cases include structures 7A−C and 13C in Figure 3. To trace the origin of this enhanced stability, we studied isosurface plots of bonding molecular orbitals associated with the edge-bound H atom.

Figure 4a is a plot for 7A, a case of unusual stability (E_{ads} = 1.26 eV), while Figure 4b is for an edge−face complex based on the pentagonal bipyramid (E_{ads} = 0.92 eV). In both cases, the s orbital of the edge-bound H is in a bonding combination with d-orbitals from the two adjacent Pd atoms making up the edge. In 7A, however, the bonding includes significant contributions from the second neighbor Pd atoms, and the bonding charge is spread over a neighboring face. These contributions are less pronounced in Figure 4b. The enhanced bonding can be linked to the geometry of 7A. The Pd−H edge is nearly coplanar with the neighboring face. This permits strong overlap of the d-orbitals from the edge Pd and the second-neighbor Pd atoms. All face−edge combinations with enhanced stability share this geometrical feature. This arrangement also gives rise to a larger charge transfer to the edge-bound H atom than for other edge-bound atoms, as can be seen in Table 3. Figure 4c shows the bonding orbital for the edge-bound H atom for 13C. The same cooperative bonding configuration as in 7A can be seen. It is interesting to note that the structure of the capped octahedron, 7A, including the placement of the H on the upper edge, appears as a part of 13C. (The atoms corresponding to the capped octahedron are shown in blue, while the remaining Pd atoms are shown in white.)

In previous calculations for large clusters and surfaces, a competition bond effect was found, wherein closely spaced adsorbate atoms bind less strongly to the substrate than well separated ones.[36] We do not see a strong proximity effect in the complexes shown in Figure 3. E_{ads} for 7A, where the H atoms are on opposites sides of the cluster (see Figure 4), is only slightly larger, by 0.02 and 0.04 eV, respectively, than for 7B and 7C where the H atoms are on adjacent sites. For 13A, where the H atoms are well separated, E_{ads} is approximately 0.1 eV larger than for 13C, where the H atoms are on adjacent faces, suggesting a possible effect. Yet many structures were considered in which the H atoms were even further apart than on 13A, on opposite sides of the cluster, and all of these were found to have smaller values of E_{ads} than 13A−C. In addition, it should be noted that in 13B, the two H atoms share one Pd neighbor in common, which would not be expected if the proximity effect were strong. Further systematic calculations would be necessary to confirm the existence of such an effect for larger clusters.

dx.doi.org/10.1021/jp403089x | J. Phys. Chem. A 2013, 117, 10407−10415

D. Adsorption Energy Trends with Cluster Size. E_{ads} vs N for molecular adsorption is shown in Figure 5a. There is a large increase between Pd_4 and Pd_7, followed by a decrease as the cluster size increases further. The value of 0.32 eV calculated for $N = 19$ is approaching the adsorption energy for H_2 on a bulk Pd surface, which was calculated to be 0.21 eV using the PBE functional.[17]

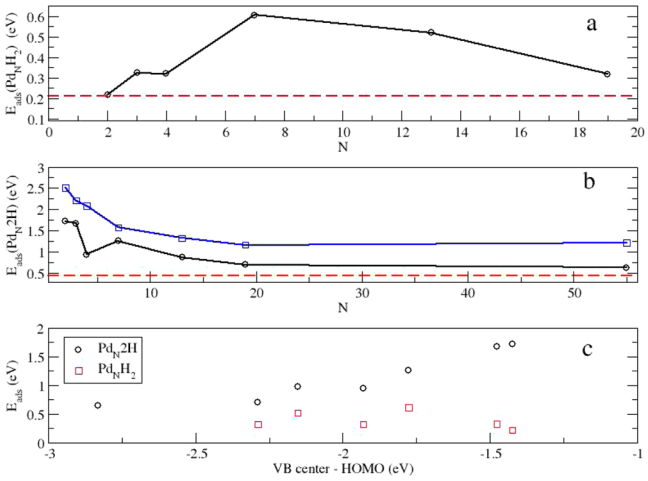

Figure 5. Adsorption energy of the most stable Pd_NH_2 (panel a) and Pd_N2H (panel b, circles) complexes versus N. The corresponding bulk values are indicated by dashed lines in each panel. Panel c plots the dissociative (2H) and molecular (H_2) adsorption energies versus the energy of the center of the valence manifold of states for each complex. See text for details.

E_{ads} for dissociative adsorption (Figure 5b) generally decreases toward the experimental bulk limit of 0.45 eV,[37] with increasing cluster size. This is consistent with the trend found in experimental measurements for Pd nanoparticles that show an increase in adsorption energy with decreasing particle size.[38] E_{ads} for Pd_4 clearly departs from the trend, appearing unusually small. One reason for this may be the lack of favorable edges on Pd_4 where binding of the sort seen in Figure 4a can occur. This may depress the adsorption energy for $N = 4$ relative to that of $N = 7$, which has a favorable edge site. Note that the largest value of E_{ads} for Pd_72H complexes that lack the favorable edge is 0.92 eV, comparable to that of Pd_42H, 0.94 eV. Another possibility involves the fact that the singlet−triplet splitting for Pd_4, 0.84 eV, is much larger than the comparable splitting between the two most stable spin states for the other Pd_N clusters considered, which are typically in the range 0.15−0.25 eV.[22] The relatively higher energy of the singlet may have the effect of driving up the energy of Pd_42H, which is also a spin singlet. The second curve in Figure 5b (with squares) shows E_{ads} corrected for the spin splitting of the bare cluster. Specifically, the plot shows $E_{ads} + (E(M^*) - E(M))$, where $E(M)$ is the total energy of the bare cluster at its ground state spin multiplicity, M, and $E(M^*)$ is the energy of the bare cluster and at the spin multiplicity of the lowest-energy Pd_N2H complex. (The curve is shifted in energy for clarity.) This corrected curve shows a smooth increase in E_{ads} with decreasing cluster size. Note that the values for both Pd_4 and Pd_2 appear adjusted in the corrected curve. The singlet−triplet splitting for Pd_2 is also relatively large, 0.49 eV. The E_{ads} vs N results show that cluster size effects can be very significant for the smallest clusters.

Previous calculations on transition metal catalysts, both for surfaces[39] and for clusters,[21,40] have shown an inverse relationship between the depth of the center of the valence d-band of states below the Fermi energy and E_{ads} for dissociative adsorption. To test this for the Pd_N2H complexes studied here, E_{ads} is plotted against the average energy of the occupied valence orbitals with respect to the energy of the highest occupied molecular orbital (HOMO) in Figure 5c. (Note that the valence states of Pd_N have a small admixture of 5s, along with their predominant 4d character. This is taken to be sufficiently small that the d-band center can be found by simply averaging the energy of the occupied valence states.) An approximately linear trend can be seen in the figure, similar to the previous calculations. It is of interest to note that this correlation disappears when E_{ads} is plotted against the absolute value of the valence band center, i.e., without the HOMO as a reference level (not shown in the figure). In this case no correlation is observed between the valence band center and the adsorption energy. This can be understood qualitatively by considering that the depth of the d-band states with respect to the HOMO is a measure of how strongly they can contribute to bonding interactions, whereas the absolute depth is a measure of the energy required to remove the electron from the cluster and is therefore not relevant to bonding.

Figure 5c also shows the molecular adsorption energy plotted versus the depth of the valence band center. Unlike the situation for dissociative adsorption, there is clearly no correlation seen in this case.

E. Adsorption Barriers. NEB calculations were carried out to gauge the existence and size of energy barriers to H_2 adsorption on Pd_N clusters. To obtain a sampling of possible adsorption pathways, we focused on the most stable sites for molecular and one-step dissociative adsorption (i.e., complexes that were obtained directly by relaxing from a starting placement of an H_2 molecule on the cluster) for each cluster size. In the case of molecular adsorption, no barriers were found for any of the complexes studied ($N = 2$−7 and 13). The reaction path is downhill in energy from the separated reactants to the molecularly adsorbed complex in each case.

For dissociative adsorption, we note that the ground state spin multiplicity of the reactants ($Pd_N + H_2$) differs from that of the product (Pd_N2H) in most cases. Thus, a nonadiabatic transition between potential energy surfaces corresponding to different spins is usually required for the system to reach the product ground state. Previous calculations for Pd_42H estimated the probability for a nonadiabatic transition from the triplet to the singlet surface to lie in the range of 0.1 to 0.4 during the approach of H_2 to the cluster.[11] This suggests that nonadiabatic transitions can occur readily near relevant surface crossing points. To determine approximate crossing points, we used NEB to independently find pathways for both the higher and lower spin states. At each point along the NEB pathway for the higher spin, we then performed a single-point energy evaluation at the lower spin and vice versa for the points along the lower spin pathway. Each of these calculations generally produces an approximate surface crossing. For determining adsorption barriers, we assume the transition to occur at the lower of the two points. We also directly compared the NEB pathways for the high spin case and low spin case using the separation of the center of mass (COM) of the Pd_N cluster and the COM of the two H atoms as the reaction coordinate. This gives another estimate of the surface crossing point. For

dx.doi.org/10.1021/jp403089x | J. Phys. Chem. A 2013, 117, 10407−10415

completeness, we also determined barrier heights for the adiabatic (spin conserved) cases.

Minimum energy pathways for dissociative adsorption on N = 7 and 13 are shown in Figure 6, with the COM separation

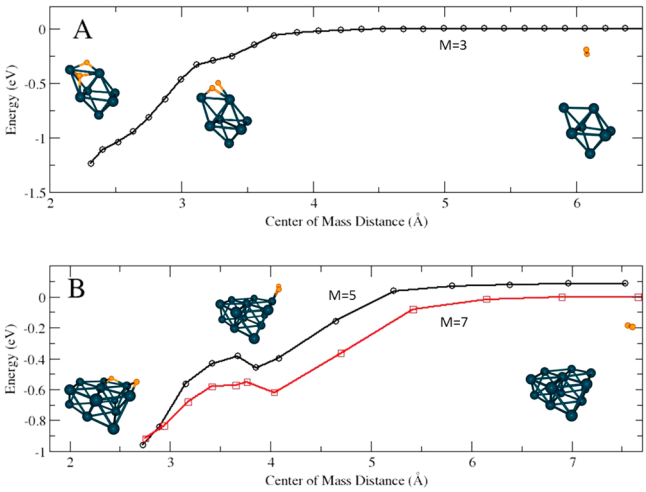

Figure 6. Minimum energy reaction pathways for dissociative adsorption of H_2 onto Pd_N clusters for N = 7 (A) and 13 (B) versus the distance between the centers of mass of the Pd_N cluster and the H_2 molecule. See text for details.

used as reaction coordinate. The circles and squares represent data for individual configurations used in the NEB calculations. In the case of H_2 dissociation on Pd_7, the ground state spin multiplicity of the reactants (M = 3) is the same as that of the products. The reaction proceeds entirely on the triplet surface and occurs without barrier (Figure 6a). There is no local minimum corresponding to molecular adsorption, although a dip in the curve can be seen around 3.4 Å.

For dissociation on the Pd_{13} cluster, Figure 6b displays the minimum energy pathways for the ground state multiplicity of the reactants (M = 7) and for that of the products (M = 5). At large COM separations (around 7 Å), the energy splitting is simply that between the bare clusters at those multiplicities (0.15 eV). On both surfaces, the minimum energy pathway includes a molecularly adsorbed intermediate state (around 4 Å) that is obtained without barrier. A small barrier of approximately 0.07 eV separates that minimum from the dissociated product. We note that the surface crossing predicted by these curves occurs very close to the product geometry. This is consistent with the crossing points predicted by performing single-point energy evaluations for the opposite spin at each NEB geometry represented on the two curves in the figure. Analogous NEB calculations have been performed to obtain dissociation pathways for Pd_N2H complexes for N = 2, 3, and 4 for the relevant spin multiplicities. In these cases, barriers of up to 0.4 eV exist, with the surface crossing points occurring either near the peak of the barrier or after the barrier. Dissociation reactions on these smaller clusters are therefore expected to proceed more slowly compared to those on larger clusters.

F. Hydrogen Atom Migration on Pd_N. NEB calculations were also done to investigate H atom migration across Pd_N cluster surfaces. In Figure 7, we show the minimum energy pathway for an H atom migrating across a Pd_7 isomer. The configuration on the left is the lowest energy one-step Pd_72H dissociation complex. The final configuration on the right is 7A,

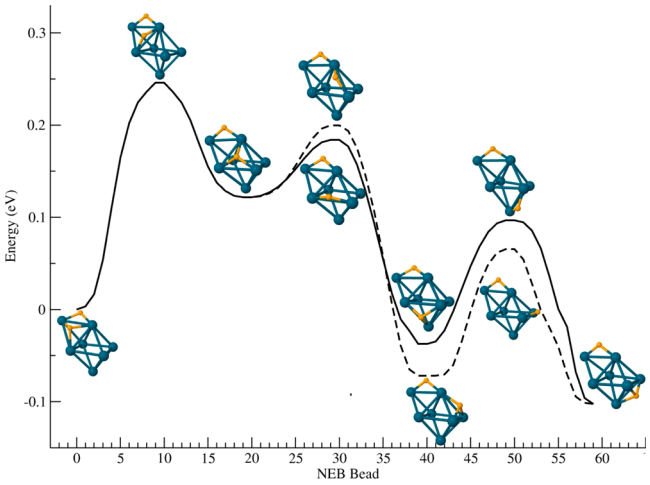

Figure 7. Minimum energy pathways for H-atom migration on Pd_7. Each tick mark on the X-axis indicates an individual bead in the NEB calculation.

the most stable Pd_72H configuration. We consider two different H atom migration pathways that lead from the initial to the final configuration. Each path consists of the H atom making a series of moves from a face site over an edge to an adjacent face. Though the energetics are somewhat different for the two paths, the overall results are very similar. The largest barrier encountered is associated with the first step and is nearly 0.25 eV. Roughly 0.15 eV of this consists of the energy difference between the local minima. Other barriers are approximately 0.07, 0.1, and 0.15 eV.

We also examined H atom migration on Pd_4 and on the pentagonal bipyramid structure for Pd_7. An H atom moving from one edge across a face to another edge in Pd_42H (structure 4C to 4B in Figure 3) had a barrier of 0.02 eV; the energy difference between the minima is 0.25 eV. On the pentagonal bipyramid structure, the motion of an H atom between adjacent faces on the same side of the cluster involved very low barriers (0.05 eV), while motion between faces on opposite sides of the cluster had a much higher barrier (0.25 eV). Earlier calculations on an octahedral Pd_62H complex using the B3LYP functional and LANL2DZ basis set give similar barrier heights (0.06−0.14 eV).[9]

Finally, we completed similar NEB calculations for Pd_{13}, examining the motion of the dissociated H atom over a section of the cluster surface. We plot the results in Figure 8, showing cluster energy vs a reaction coordinate taken to be the H−H separation. The kink in the curve near 3 Å is related to changes in Pd−Pd bond lengths near the migrating H atom. The barrier heights found for Pd_{13} are approximately 0.01−0.20 eV. This range is very similar to that found for Pd_7. Also similar to Pd_72H is the fact that the largest diffusion barrier is associated with the lowest energy $Pd_{13}2H$ configuration that occurs as a result of the direct dissociation of an H_2 dimer placed on the surface. The similarity in the results for Pd_7 and Pd_{13}, i.e., barrierless dissociation and small diffusion barriers for dissociated H atoms, suggest that similar results can be expected for larger clusters.

IV. SUMMARY

We presented the results of systematic DFT calculations of both molecular and dissociative adsorption of single H_2 molecules on low-energy Pd_N cluster isomers (N = 2−4, 7,

dx.doi.org/10.1021/jp403089x | J. Phys. Chem. A 2013, 117, 10407−10415

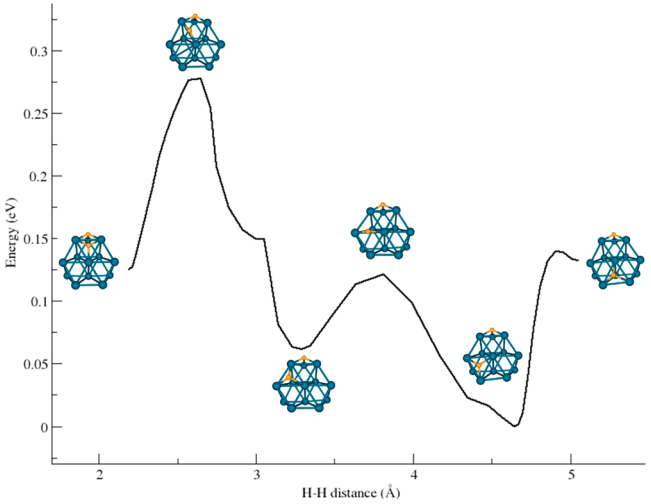

Figure 8. Minimum energy pathways for H-atom migration on Pd_{13}.

13, 19, and 55), using the PBE0 functional and the Stuttgart cc-PVDZ-pp basis set. This combination was found to reproduce experimental results for Pd-based test systems particularly well. Optimal structures for Pd_NH2 and Pd_N2H complexes were determined for sizes up to $N = 13$. Additional calculations were done to investigate dissociative adsorption on $N = 19$ and 55. Molecular adsorption of H_2 occurs without barrier for all cluster sizes with the H_2 molecule binding exclusively at atop sites and making two Pd−H bonds. No change in the ground state spin multiplicity of the cluster is found as a result of molecular adsorption, and only a very small transfer of electron charge from Pd_N to the H atoms. Molecular adsorption energies were largest for $N = 7$ and 13. For a given Pd_N isomer, the largest molecular adsorption energies were generally found at the Pd sites with the smallest coordination. For dissociative adsorption, the binding of H atoms to 3-fold face sites was generally preferred in the most stable complexes; however, enhanced binding was found for certain edge sites due to geometrical factors that promote an increased involvement of second-neighbor Pd atoms in the bonding. Electron charge is transferred from the Pd_N cluster to the H atoms in all Pd_N2H complexes. Barriers to dissociative adsorption were investigated and found to depend on cluster size. In the larger clusters, dissociation was found to be barrierless, while barriers of up to 0.4 eV are found for the smallest clusters. Computed barriers to the migration of dissociated H atoms between neighboring minima were found to span an energy range from 0.02 to 0.25 eV.

There are many interesting questions regarding the structure and reactivity of Pd_N clusters as nanoscale catalysts.[41−44] The results presented here provide insight into likely initial steps involved in the synthesis of H_2O_2 from H_2 and O_2 over Pd_N. Further questions related to this reaction include the effect of H coverage on the energetics of reaction steps, O_2 reactivity and coverage effects, the formation of reaction intermediates, and H_2O_2 desorption. We are currently studying these issues.

■ ASSOCIATED CONTENT

Ⓢ Supporting Information

Coordinates for all of the Pd_N clusters and hydrogenated complexes. This material is available free of charge via the Internet at http://pubs.acs.org.

■ AUTHOR INFORMATION

Corresponding Authors

*(A.W.P.) E-mail: adam.pelzer@northwestern.edu.
*(K.A.J.) E-mail: jackslka@cmich.edu.
*(J.J.) E-mail: jellinek@anl.gov. Tel: 773-209-5501.

Notes

The authors declare no competing financial interest.

■ ACKNOWLEDGMENTS

The authors gratefully acknowledge CMU undergraduate student Katelyn Montgomery for her assistance with aspects of this project. A.P. and K.A.J. were supported by the U.S. Department of Energy under Award No. DE-SC0001330. J.J. was supported by the Office of Basic Energy Sciences, Division of Chemical Sciences, Geosciences and Biosciences, U.S. Department of Energy, under Contract No. DE-AC02-06CH11357, and by the Institute for Atom-efficient Chemical Transformations (IACT), an Energy Frontier Research Center funded by the U.S. Department of Energy, Office of Science, Office of Basic Energy Sciences.

■ REFERENCES

(1) Wells, D. H.; Delgass, W. N.; Thomson, K. T. Formation of Hydrogen Peroxide from H_2 and O over a Neutral Gold Trimer: A DFT Study. *J. Catal.* **2004**, *225*, 69−77.

(2) Joshi, A. M.; Delgass, W. N.; Thomson, K. T. Investigation of Gold−Silver, Gold−Copper, and Gold−Palladium Dimers and Trimers for Hydrogen Peroxide Formation from H_2 and O_2. *J. Phys. Chem. C* **2007**, *111*, 7384−7395.

(3) Landon, P.; Collier, J.; Carley, A. F.; Chadwick, D.; Papworth, A. J.; Burrows, A.; Kiely, C. J.; Hutchings, G. J. Direct Synthesis of Hydrogen Peroxide from H_2 and O_2 Using Pd and Au Catalysts. *Phys. Chem. Chem. Phys.* **2003**, *5*, 1917−1923.

(4) Edwards, J. K.; Solsona, B. E.; Landon, P.; Carley, A. F.; Herzing, A.; Kiely, C. J.; Hutchings, G. J. Direct Synthesis of Hydrogen Peroxide from H_2 and O_2 Using TiO_2-Supported Au−Pd catalysts. *J. Catal.* **2005**, *236*, 69−79.

(5) Efremenko, I.; German, E. D.; Sheintuch, M. Density Functional Study of the Interactions between Dihydrogen and Pd_n (n = 1−4) Clusters. *J. Phys. Chem. A* **2000**, *104*, 8089−8096.

(6) Cui, Q.; Musaev, D. G.; Morokuma, K. Molecular Orbital Study of H_2 and CH_4 Activation on Small Metal Clusters. I. Pt, Pd, Pt_2, and Pd_2. *J. Chem. Phys.* **1998**, *108*, 8418−8428.

(7) Moc, J.; Musaev, D. G.; Morokuma, K. Adsorption of Multiple H_2 Molecules on Pd_3 and Pd_4 Clusters. A Density Functional Study. *J. Phys. Chem. A* **2000**, *104*, 11606−11614.

(8) Cui, Q.; Musaev, D. G.; Morokuma, K. Molecular Orbital Study of H_2 and CH_4 Activation on Small Metal Clusters. 2. Pd_3 and Pt_3. *J. Phys. Chem. A* **1998**, *102*, 6373−6384.

(9) Wang, Y.; Cao, Z.; Zhang, Q. Density Functional Study of Multiple H_2 Adsorption and Activation on a Pd_6 Cluster. *Chem. Phys. Lett.* **2003**, *376*, 96−102.

(10) Barone, G.; Duca, D.; Ferrante, F.; La Manna, G. CASSCF/CASPT2 Analysis of the Fragmentation of H_2 on a Pd_4 Cluster. *Int. J. Quantum Chem.* **2010**, *110*, 558−562.

(11) German, E. D.; Efremenko, I.; Sheintuch, M. Hydrogen Interactions with a Pd_4 Cluster: Triplet and Singlet States and Transition Probability. *J. Phys. Chem. A* **2001**, *105*, 11312−11326.

(12) Ni, M.; Zeng, Z. Density Functional Study of Hydrogen Adsorption and Dissociation on Small Pd_n (n = 1−7) clusters. *J. Mol. Struct.* **2009**, *910*, 14−19.

(13) Paul, J. F.; Sautet, P. Density-Functional Periodic Study of the Adsorption of Hydrogen on a Palladium (111) Surface. *Phys. Rev. B* **1996**, *53*, 8015−8027.

(14) Dong, W.; Ledentu, V.; Sautet, P.; Eichler, A.; Hafner, J. Hydrogen Adsorption on Palladium: a Comparative Theoretical Study of Different Surfaces. *Surf. Sci.* **1998**, *411*, 123−136.
(15) Lovvik, O. M.; Olsen, R. A. Adsorption Energies and Ordered Structures of Hydrogen on Pd(111) from Density-Functional Periodic Calculations. *Phys. Rev. B* **1998**, *58*, 10890−10898.
(16) Lober, R.; Hennig, D. Interaction of Hydrogen with Transition Metal fcc(111) Surfaces. *Phys. Rev. B* **1997**, *55*, 4761−4765.
(17) Dong, W.; Hafner, J. H_2 Dissociative Adsorption on Pd(111). *Phys. Rev. B* **1997**, *56*, 15396−15403.
(18) Resch, C.; Berger, H. F.; Rendulic, K. D.; Bertel, E. Adsorption Dynamics for the System Hydrogen/Palladium and Its Relation to the Surface Electronic Structure. *Surf. Sci.* **1994**, *316*, L1105−L1109.
(19) Mitsui, T.; Rose, M. K.; Fomin, E.; Ogletree, D. F.; Salmeron, M. Hydrogen Adsorption and Diffusion on Pd(111). *Surf. Sci.* **2003**, *540*, 5−11.
(20) Mitsui, T.; Rose, M. K.; Fomin, E.; Ogletree, D. F.; Salmeron, M. Dissociative Hydrogen Adsorption on Palladium Requires Aggregates of Three or More Vacancies. *Nature* **2003**, *422*, 705−707.
(21) Lee, H.-W.; Chang, C.-M. Size Effect of Pd clusters on Hydrogen Adsorption. *J. Phys: Condens. Matter* **2011**, *23*, 045503−1−045503−5.
(22) In preparation.
(23) Valiev, M.; Bylaska, E.; Govind, N.; Kowalski, K.; Straatsma, T.; van Dam, H.; Wang, D.; Nieplocha, J.; Apra, E.; Windus, T.; de Jong, W. A. NWChem: A Comprehensive and Scalable Open-Source Solution for Large Scale Molecular Simulations. *Comput. Phys. Commun.* **2010**, *181*, 1477−1489.
(24) Jules, J. L.; Lombardi, J. R. Transition Metal Dimer Internuclear Distances from Measured Force Constants. *J. Phys. Chem. A* **2003**, *107*, 1268−1273.
(25) Scheer, M.; Brodie, C. A.; Bilodeau, R. C.; Haugen, H. K. Laser Spectroscopic Measurements of Binding Energies and Fine-Structure Splittings of Co^-, Ni^-, Rh^-, and Pd^-. *Phys. Rev. A* **1998**, *58*, 2051−2062.
(26) Gingerich, K. A. On the Equilibrium between Monatomic and Diatomic Palladium and the Appearance of Potential of Pd_2. *Naturweiss* **1967**, *54*, 43.
(27) Ho, J.; Ervin, K. M.; Polak, M. L.; Gilles, M. K.; Lineberger, W. C. A Study of the Electronic Structures of Pd^-_2 and Pd_2 by Photoelectron Spectroscopy. *J. Chem. Phys.* **1991**, *95*, 4845−4853.
(28) Ishikawa, T. Photoionization Spectra of Pd in High Rydberg State. *Jpn. J. Appl. Phys.* **1993**, *32*, 4779−4780.
(29) Gantefor, G.; Gausa, M.; Meiwes-Broer, K-H; Lutz, H. O. Photoelectron Spectroscopy of Silver and Palladium Cluster Anions: Electron Delocalization versus Localization. *J. Chem. Soc., Faraday Trans.* **1990**, *86*, 2483−2488.
(30) Tolbert, M. A.; Beauchamp, J. L. Homolytic and Heterolytic Bond Dissociation Energies of the Second Row Group 8, 9, and 10 Diatomic Transition-Metal Hydrides: Correlation with Electronic Structure. *J. Phys. Chem.* **1986**, *90*, 5015−5022.
(31) Knight, L. B.; Weltner, W. Hyperfine Interaction and Chemical Bonding in the PdH Molecule. *J. Mol. Spectrosc.* **1971**, *40*, 317−327.
(32) Henkelman, G.; Uberuaga, B.; Jonsson, H. A Climbing Image Nudged Elastic Band Method for Finding Saddle Points and Minimum Energy Paths. *J. Chem. Phys.* **2000**, *113*, 9901−9904.
(33) Henkelman, G.; Jonsson, H. Improved Tangent Estimate in the Nudged Elastic Band Method for Finding Minimum Energy Paths and Saddle Points. *J. Chem. Phys.* **2000**, *113*, 9978−9985.
(34) Sheppard, D.; Henkelman, G. Paths to Which the Nudged Elastic Band Converges. *J. Comput. Chem.* **2011**, *32*, 1769−1771.
(35) Weinhold, F.; Landis, C. R. *Valency and Bonding: A Natural Bond Orbital Donor-Acceptor Perspective*; University Press: Cambridge, U.K., 2005.
(36) Alavi, A.; Hu, P.; Deutsch, T.; Silvestrelli, P. L.; Hutter, J. CO Oxidation on Pt(111): An ab Initio Density Functional Theory Study. *Phys. Rev. Lett.* **1998**, *80*, 3650−3653.
(37) Conrad, H.; Ertl, G.; Latta, E. Adsorption of Hydrogen on Palladium Single Crystal Surfaces. *Surf. Sci.* **1974**, *41*, 435−446.
(38) Huang, S.-Y.; Huang, C.-D.; Chang, B.-T.; Yeh, C.-Y. Chemical Activity of Palladium Clusters: Sorption of Hydrogen. *J. Phys. Chem. B* **2006**, *110*, 21783−21787.
(39) Hammer, B.; Norskov, J. K. Electronic Factors Determining the Reactivity of Metal Surfaces. *Surf. Sci.* **1995**, *343*, 211−220.
(40) Tang, W.; Henkelman, G. Charge Redistribution in Core−Shell Nanoparticles to Promote Oxygen Reduction. *J. Chem. Phys.* **2009**, *130*, 194504.
(41) Kumar, V.; Kawazoe, Y. Icosahedral Growth, Magnetic Behavior, and Adsorbate-Induced Metal-Nonmetal Transition in Palladium Clusters. *Phys. Rev. B* **2002**, *66*, 144413.
(42) Koster, A. M.; Calaminici, P.; Orgaz, E.; Roy, D. R.; Reveles, J. U.; Khanna, S. N. On the Ground State of Pd_{13}. *J. Am. Chem. Soc.* **2011**, *133*, 12192.
(43) Sing, A. K.; Ribas, M. A.; Yakobson, B. I. H-Spillover through the Catalyst Saturation: An Ab Initio Thermodynamics Study. *ACS Nano* **2009**, *3*, 1657−1662.
(44) Reveles, J. U.; Koster, A. M.; Calaminici, P.; Khanna, S. N. Structural Changes of Pd_{13} upon Charging and Oxidation/Reduction. *J. Chem. Phys.* **2012**, *136*, 114505.